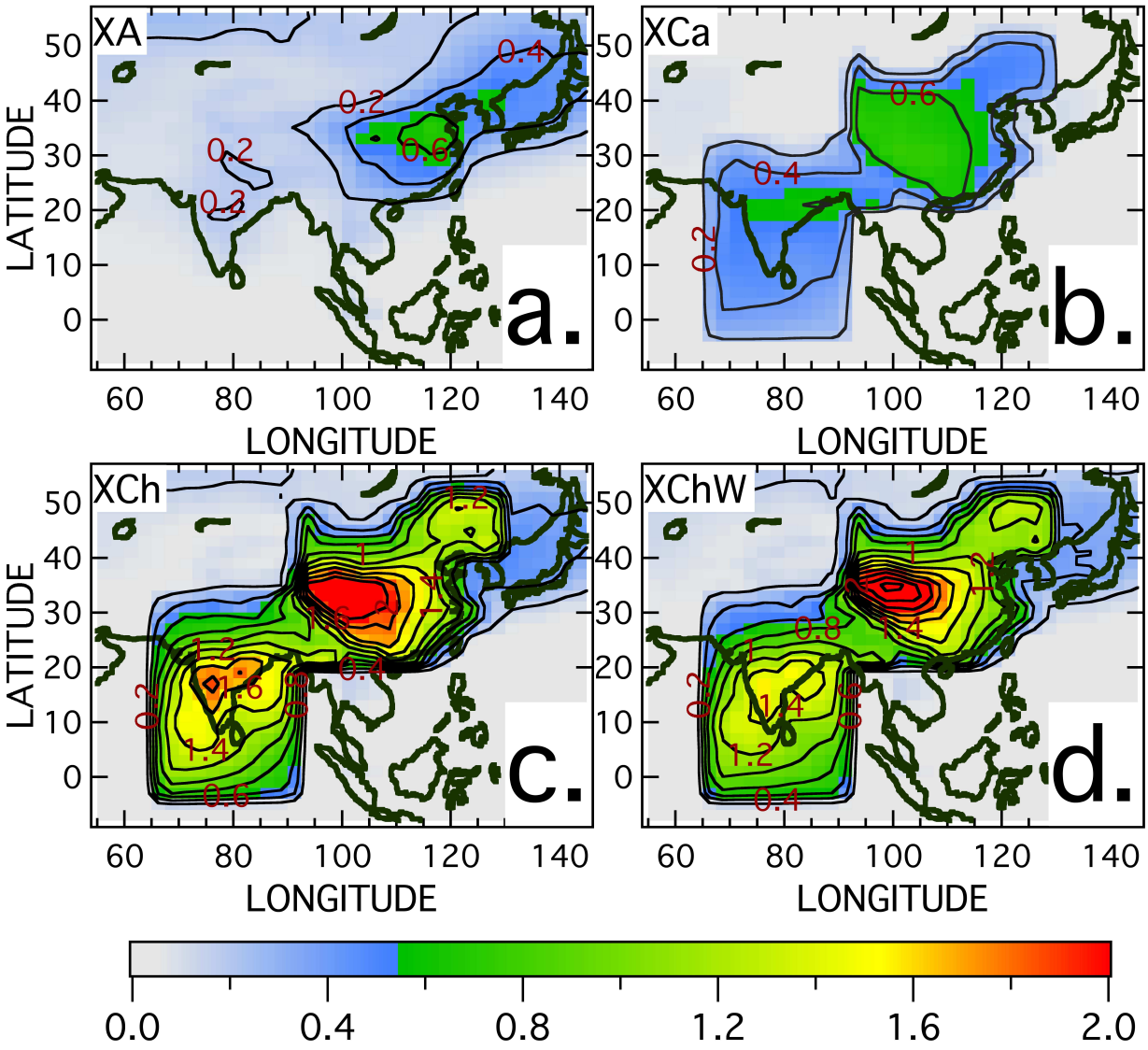

Figure 1. Column-integrated aerosol optical depth for each experiment differenced with respect to the BASE case ($\Delta\tau_a$): (a) XA, (b) XCa , (c) XCh, and (d) XChW. Note that this optical depth represents only the anthropogenic (BC, OC and SO_4) aerosol component (increase between 1950 and 1990) since the natural (dust and sea salt) component is shared with the BASE case. The contour interval is 0.2.

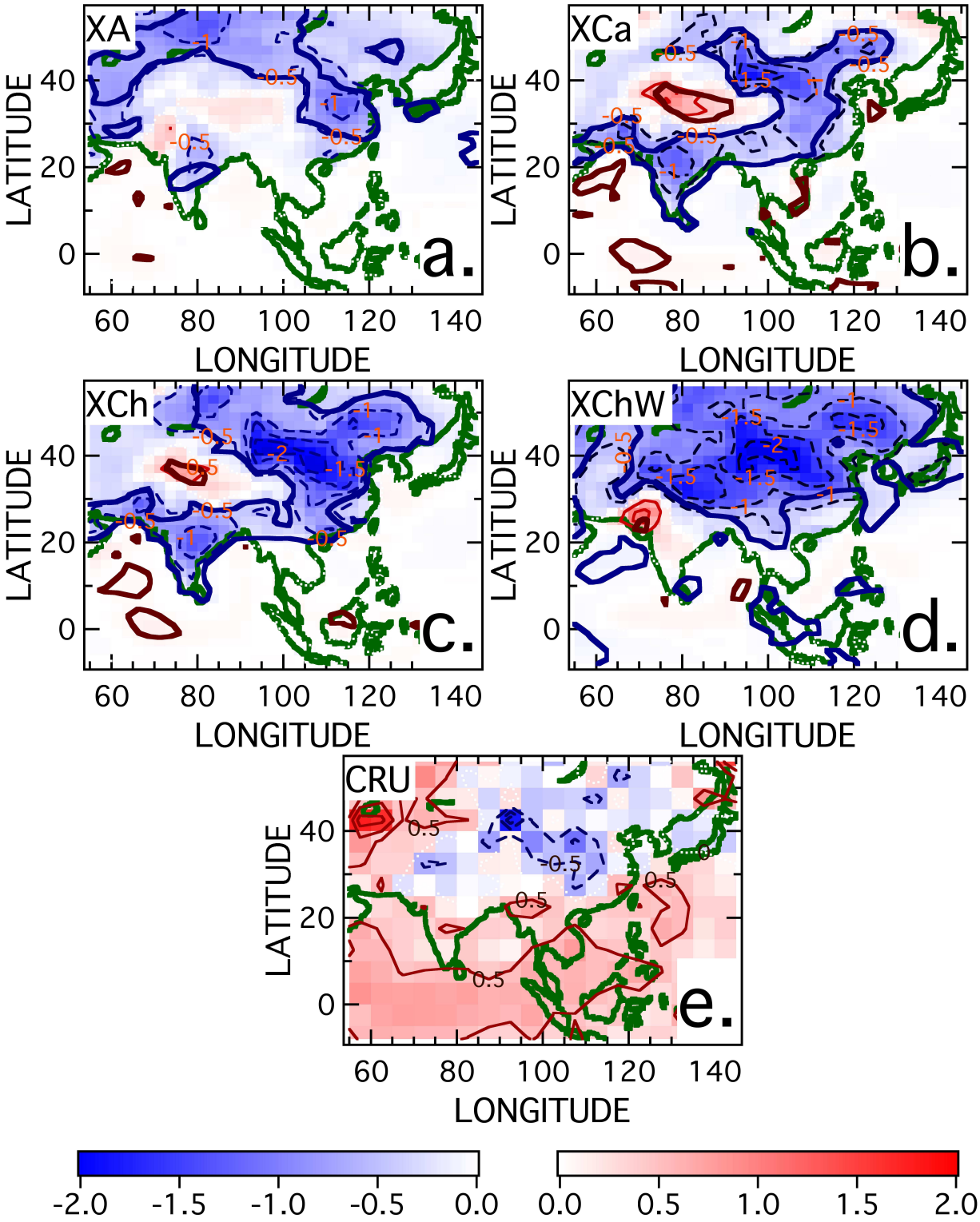

Figure 2. JJA change in surface air temperature (ΔT_s) [K] between the BASE case and (a) XA, (b) XCa, (c) XCh, and (d) XChW. (e) Observed mean ΔT_s between the 1945-1955 and 1985-1995 decades from the CRU database [*Brohan et al.*, 2006]. Thin, solid (dashed) lines and red (blue) shading indicate positive (negative) ΔT_s (contour interval 0.5 K). Thick blue and red contours enclose regions where ΔT_s is at or above the 90% confidence level.

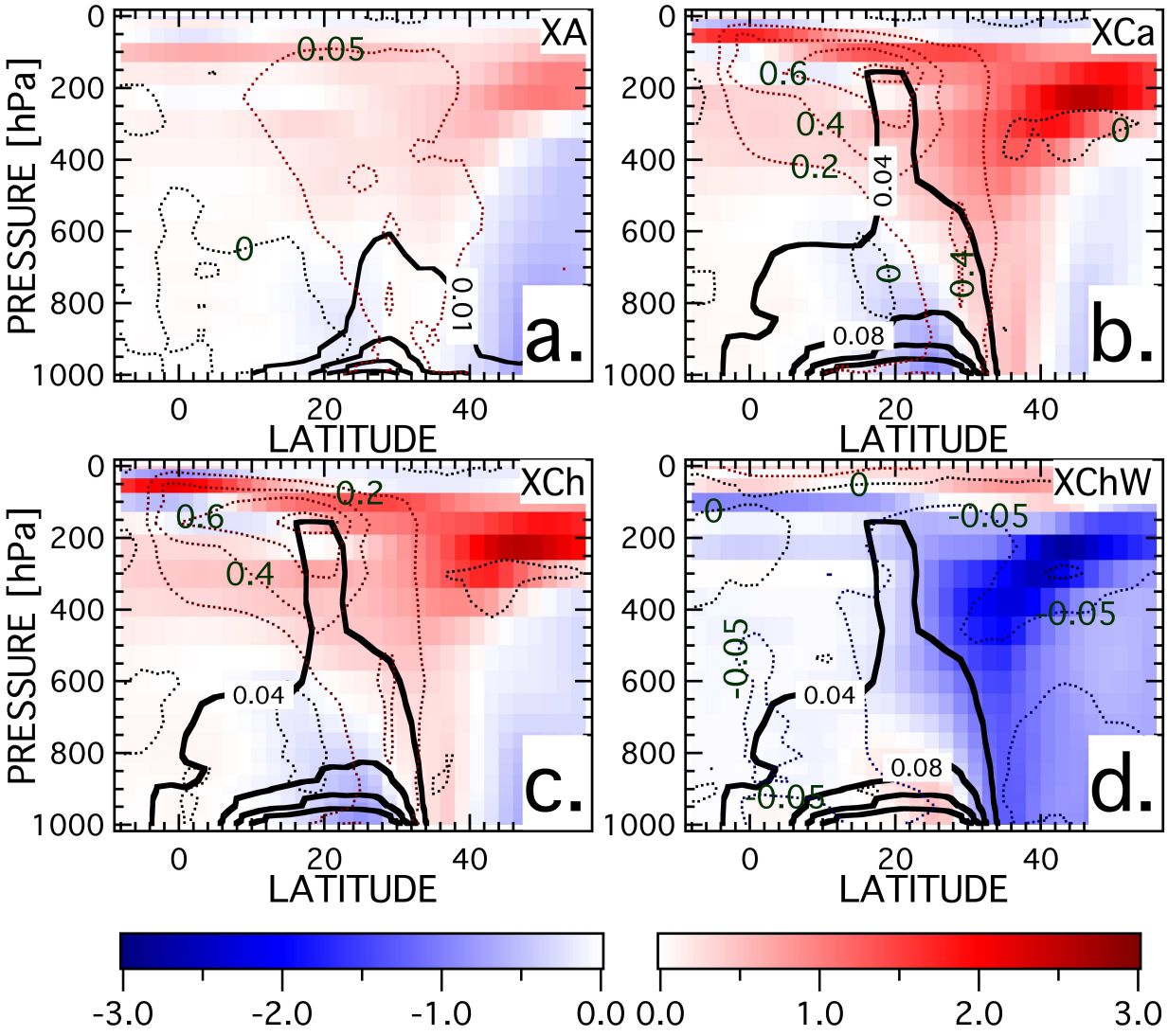

Figure 3. Zonally averaged change in JJA atmospheric temperature (ΔT_{atm}) [K] (shaded) over India (65°E-90°E) between the BASE case and (a) XA, (b) XCa, (c) XCh, and (d) XChW. Change in BC mixing ratio relative to the BASE case (thick black contours) with contour interval of 0.01 and 0.04 μg m^{-3} for XA and the HOD experiments, respectively. Thin, dotted contours indicate the change in shortwave heating rate [K d^{-1}] relative to the BASE case with contour interval of 0.05 K d^{-1} for XA and XChW and 0.2 K d^{-1} for XCa and XCh.

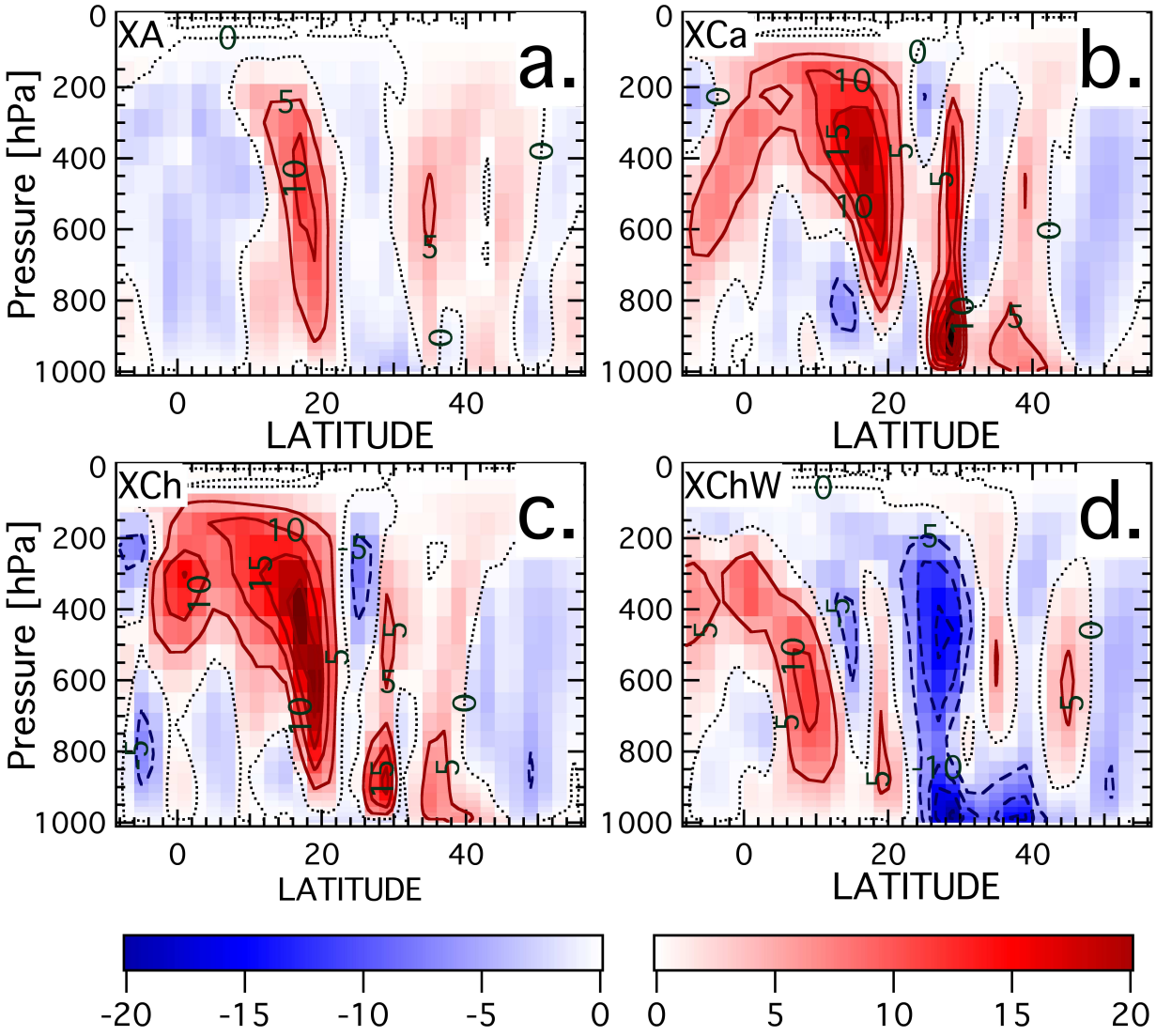

Figure 4. Zonally averaged JJA change in vertical velocity ($\Delta(-w) = \Delta\frac{-dp}{dt}$) between the BASE case and experiments over India (65°E-90°E) for (a) XA, (b) XCa, (c) XCh, and (d) XChW. Note that the negative of the vertical pressure velocity is taken such that red indicates increased vertical motion and blue indicates relative subsidence. The contour interval is 5×10^{-5} hPa s^{-1}.

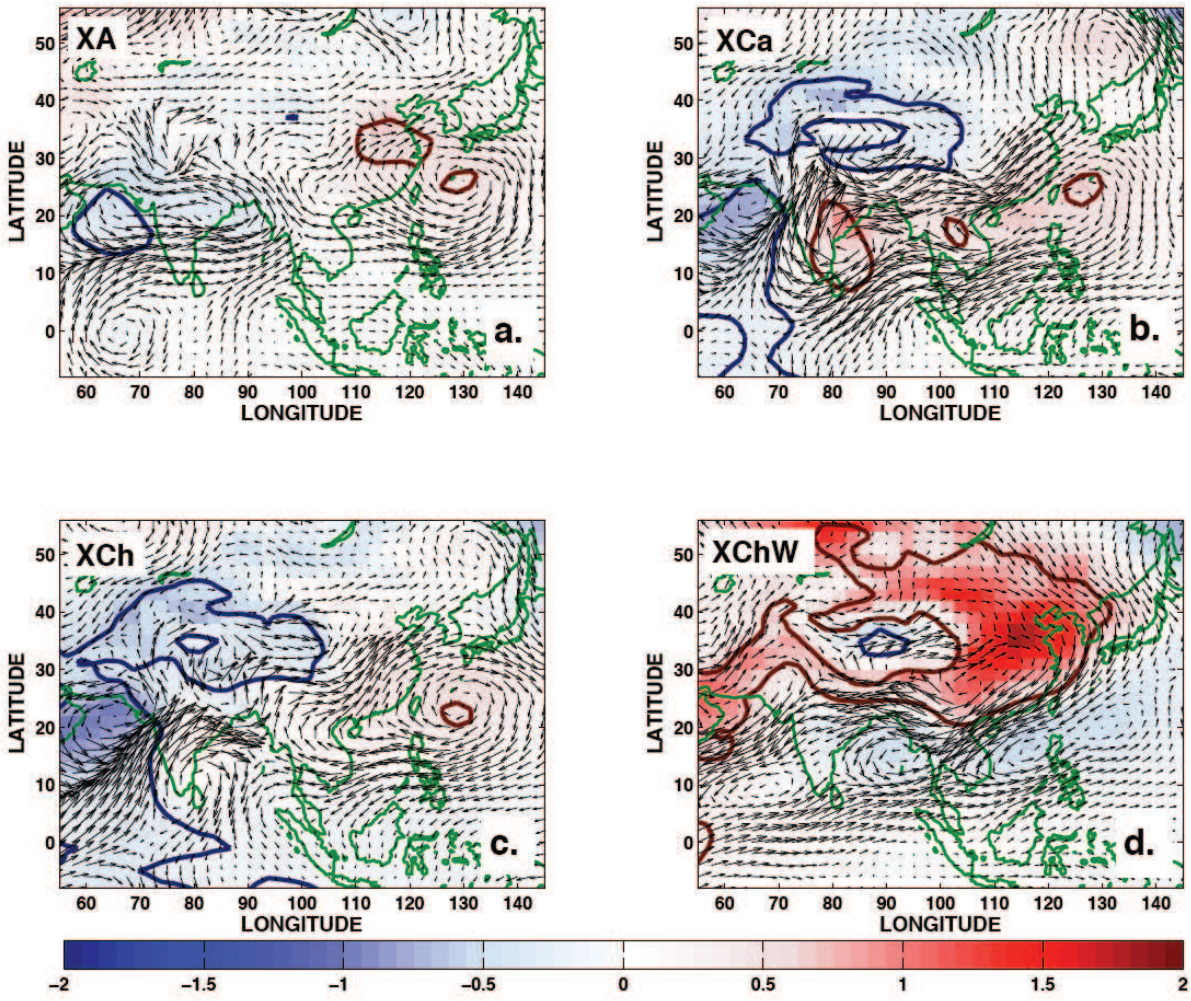

Figure 5. Change in JJA surface pressure (ΔP_{sfc}) [hPa] relative to the BASE case (shaded) for (a) XA, (b) XCa, (c) XCh, and (d) XChW. Thick blue and red contours enclose regions where ΔP_{sfc} is at or above the 90% confidence level. Changes in the 850 hPa winds relative to the BASE case are plotted as vectors.

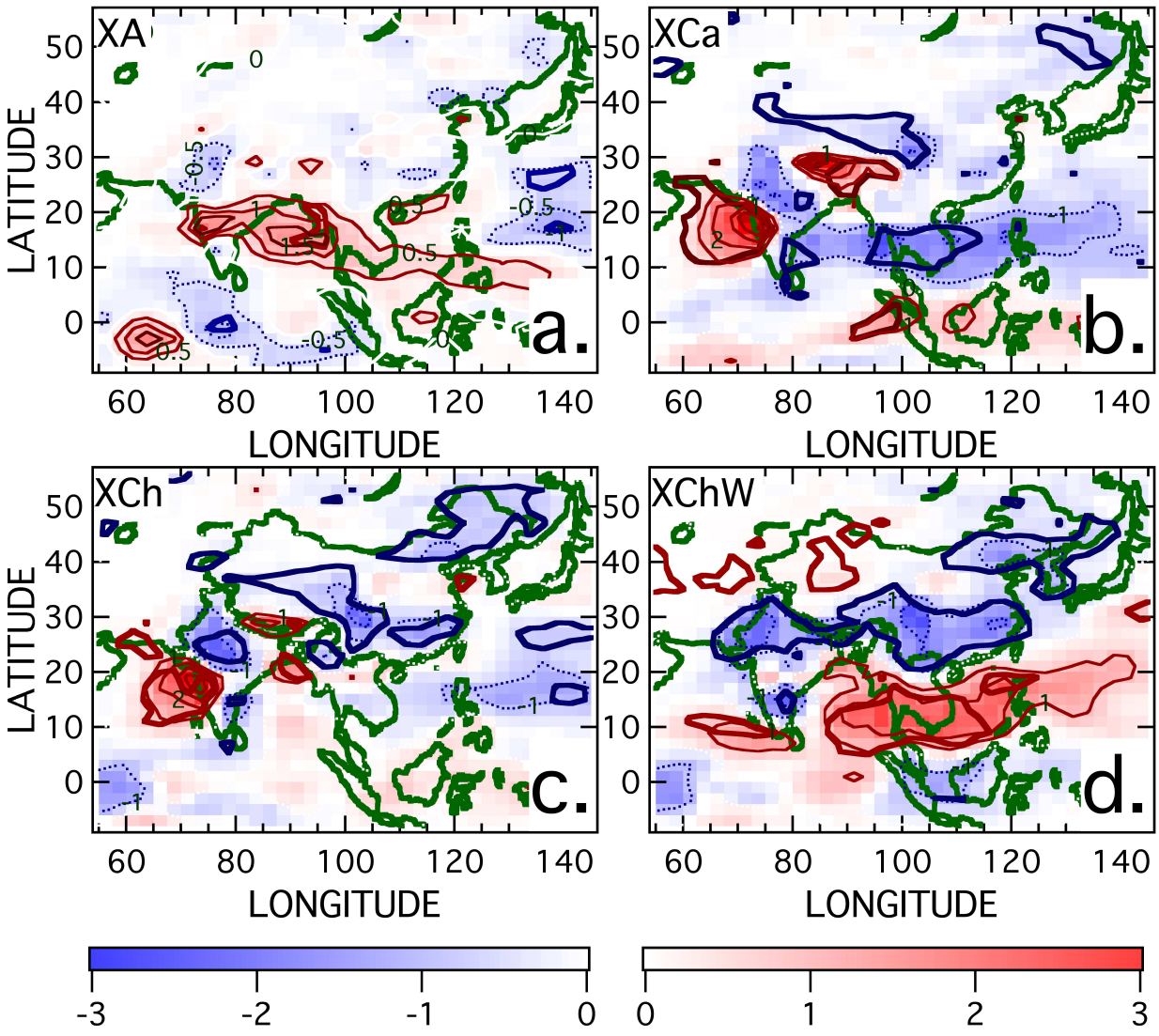

Figure 6. Change in JJA precipitation rate (ΔP) relative to the BASE case for (a) XA, (b) XCa, (c) XCh, and (d) XChW. Thin, solid (dotted) contours and red (blue) shading indicate positive (negative) ΔP (contour interval of 0.5 and 1 mm d^{-1} for XA and the HOD experiments, respectively). Thick red and blue contours inclose regions where ΔP is at or above the 90% confidence level.

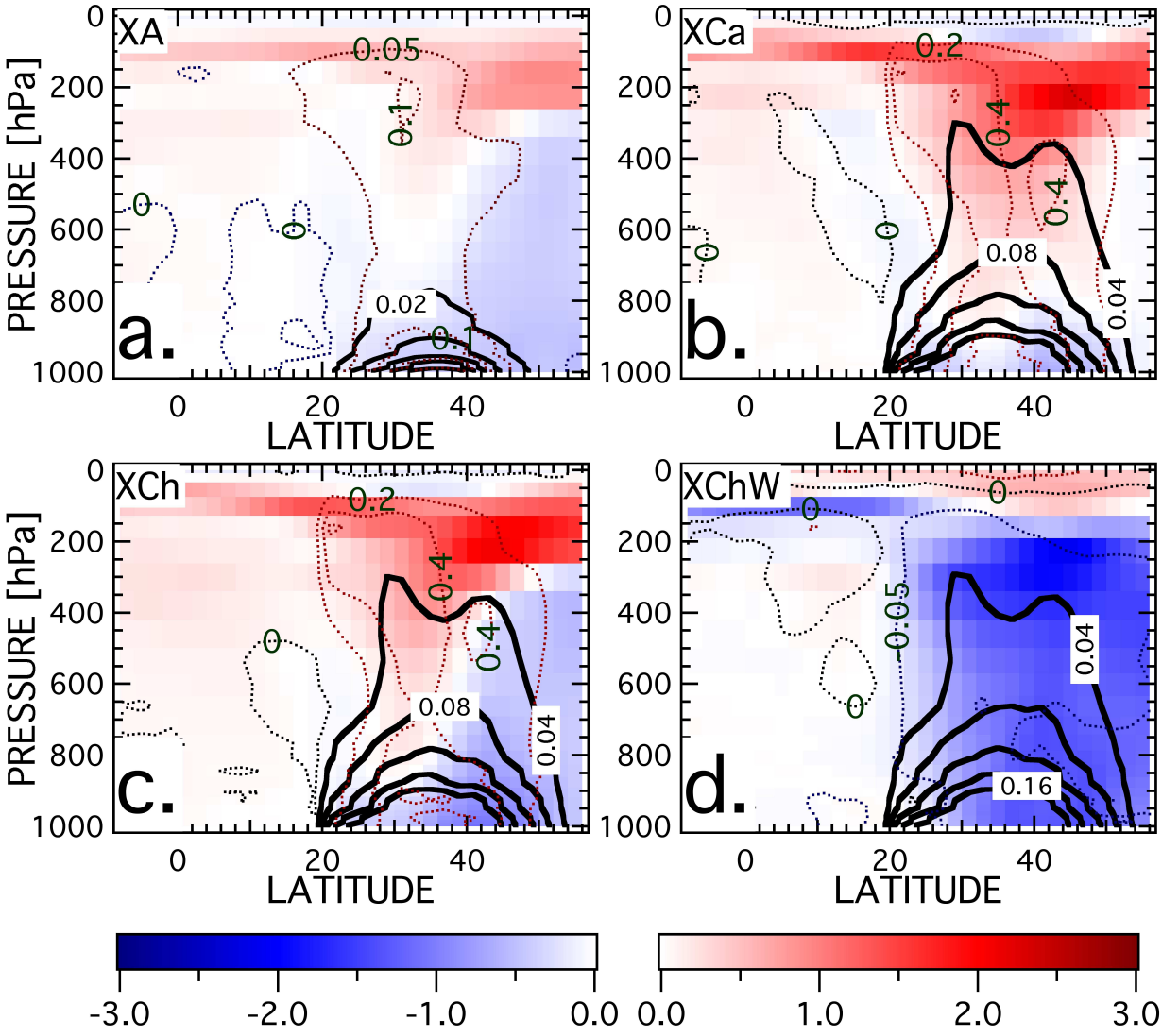

Figure 7. Same as Figure 3 (color version; ΔT_{atm}, BC mixing ratio change, and shortwave heating rate change) except zonally averaged over China (90°E-130°E).

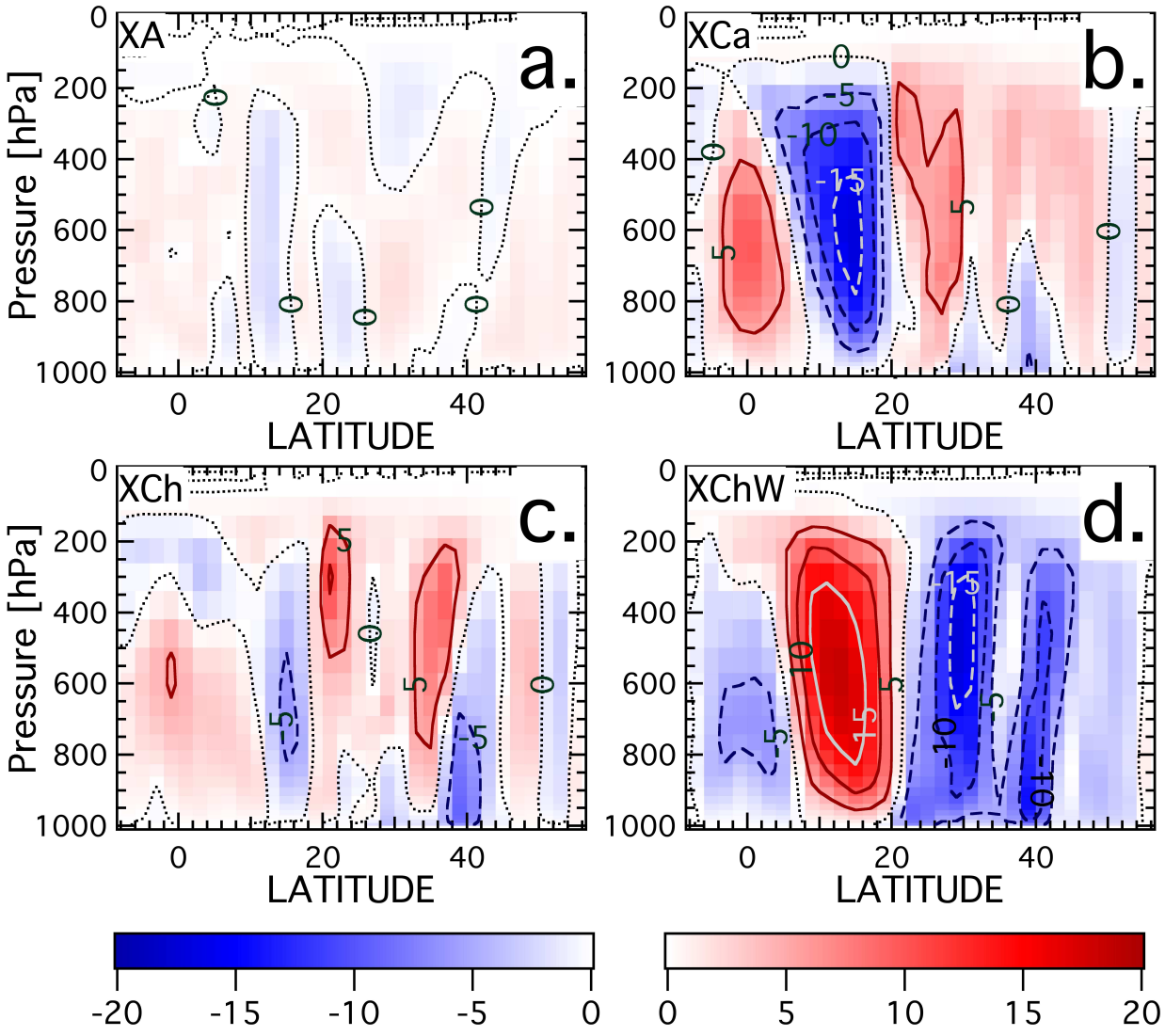

Figure 8. Same as Figure 4 (color version; $\Delta(-w) = \Delta\frac{-dp}{dt}$; contour interval 5×10^{-5} hPa s^{-1}) except zonally averaged over China (90°E-130°E)

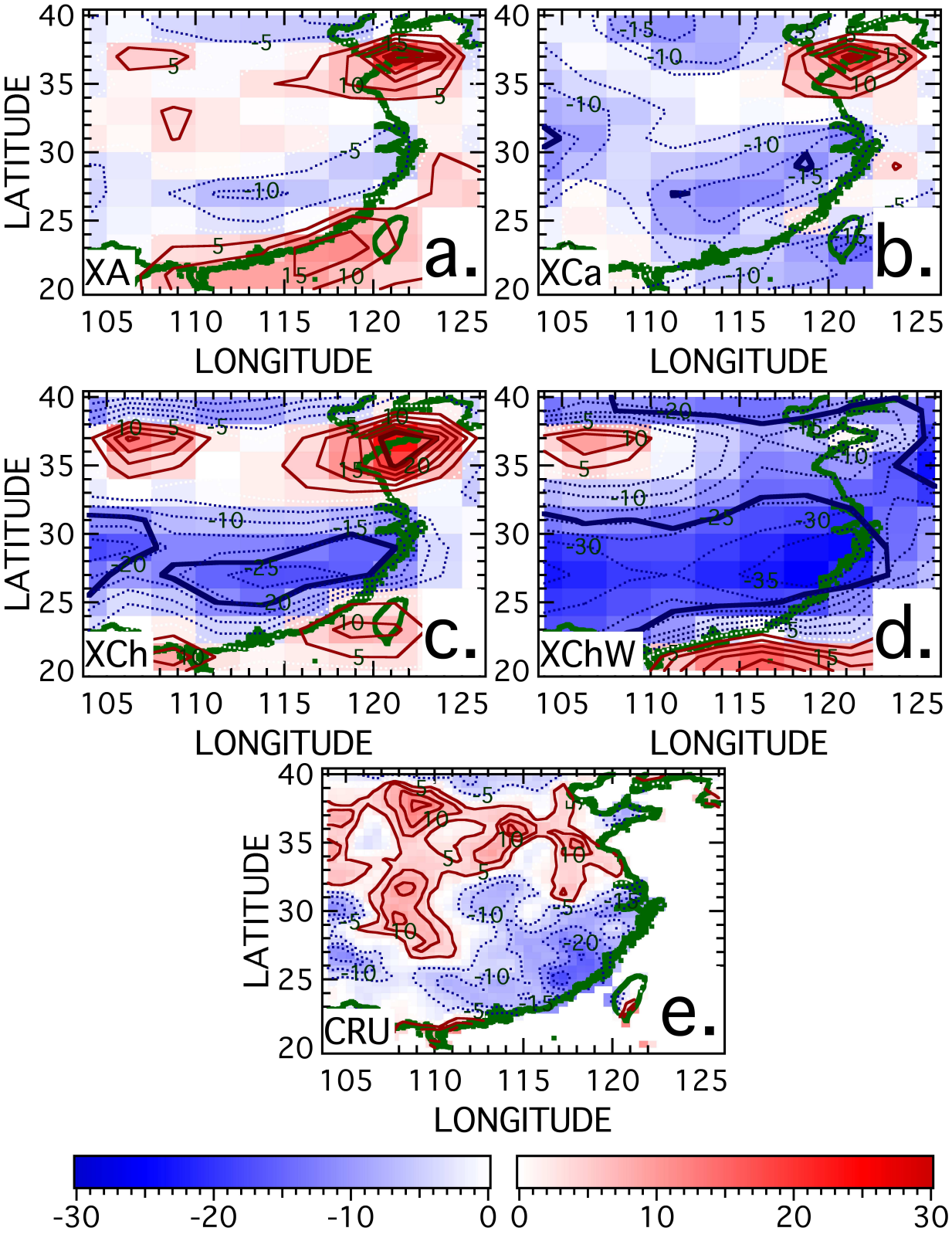

Figure 9. Percent change in total precipitation rate relative to the BASE case ((EXP-BASE)/BASE) × 100 over China for: (a) XA, (b) XCa, (c) XCh, and (d) XChW. (e) Observed percent change in total precipitation between the 1985-1995 decade and the 1945-1955 decade from the CRU database [*Brohan et al.*, 2006]. Solid (dotted) contours and red (blue) shading indicate increased (decreased) precipitation (5% contour interval). Thick blue and red contours enclose regions where the change in precipitation is at or above the 90% confidence level.